International Journal of Research
Available at https://edupediapublications.org/journals
e-ISSN: 2348-6848
p-ISSN: 2348-795X
Volume 04 Issue-17
December 2017

Simulation and Analysis of Flyback Ccm Inverter with Ic Technique Forpv System based Discrete-Time Repetitive Control

G.Poorna & T.Vinay Kumar
[1]Assistant Professor, EEE department, Bhoj Reddy Engineering College for Women
[2]Assistant Professor, EEE department, Bhoj Reddy Engineering College for Women

Abstract: *In this project we are implementing the discrete-time repetitive controller (RC) during the continuous conduction mode of operation is applied for the PV source. In this paper we use the IC technique; it is used to track the maximum power point of the PV source. MPPT can minimize the system cost and maximize the array efficiency. The proposed system is simple and cost effective. According to the comparison to the conventional controller and the repetitive controller it is obtain as a good tracking ability and disturbance rejection which is applied to fly back inverter during CCM operation. The IC algorithm was designed to control the duty cycle of Buck Boost converter and to ensure the MPPT work at its maximum efficiency. Therefore, according to the Conventional controller results which is shown that it is poor control performance because of it effect of the right-half-plane zero during the CCM operation. Which also allow the tracking and rejection of periodic signals within a specified frequency range the RC scheme by utilizing the low-pass filter. Here the stability of the closed loop system has been derived and zero tracking error will be achieved along with the stability of the closed loop system. By using the simulation results we can analyze the proposed method.*

Index Terms—Module-integrated converter, right-half-plane zero, low-pass filter, phase-lead compensation, increment condition.

INTRODUCTION

The feedback of the output current and the use of repetitive control algorithm are proposed in this paper for a fly back inverter that operates in CCM. The conventional controller consists of a linear controller and a feed forward controller. By using the conventional controller, we get the poor control accuracy due to the RHP zero which limits the available controller bandwidth.

Nowadays an AC photovoltaic (PV) system has been used mostly comparing to conventional centralized PV systems. The AC PV module system provides independent operation for each individual PV module; this design allows all modules to operate at their maximum power point (MPP) and reduces power losses caused by PV module. The AC PV module system is more reliable and easier to maintain than are centralized PV systems [1].

In the AC PV module system, to ensure maximum power extract and to provide the power to the utility grid a module-integrated converter (MIC) is attached to a single PV panel. The acceptability of the MIC is evaluated by conversion efficiency, harmonic of output current, cost, and reliability. To meet these requirements, a single-stage flyback inverter topology with an unfolding circuit has been widely used due to its number of components and its potential for high efficiency and reliability [6, 7].

The flyback inverter in DCM imposes high current stress on devices; it results in decrease of conversion efficiency. In addition, the filter design becomes difficult due to the high current ripple. Compared to the DCM flyback inverters, the CCM flyback inverter has many advantages such as higher efficiency with lower current stress, easier filter design, and lower electromagnetic interference (EMI).

To track a periodic signal and to eliminate periodic disturbance in dynamic systemsthe repetitive controller is widely used. In the repetitive control scheme, the present control input is obtained, and this operation is performed repetitively. Hence, the repetitive controller generates the control input that ensures zero tracking error [2]. In the repetitive control scheme, a low-pass filter is used to disable the learning at high-frequency so that it allows tracking/rejecting periodic signals within a specified frequency range.

PROBLEM FORMULATION AND PRELIMINARY

Averaged model of flyback inverter in CCM operation

The circuit outline of the flyback inverter is appeared in Fig. 1.

International Journal of Research
Available at https://edupediapublications.org/journals
e-ISSN: 2348-6848
p-ISSN: 2348-795X
Volume 04 Issue-17
December 2017

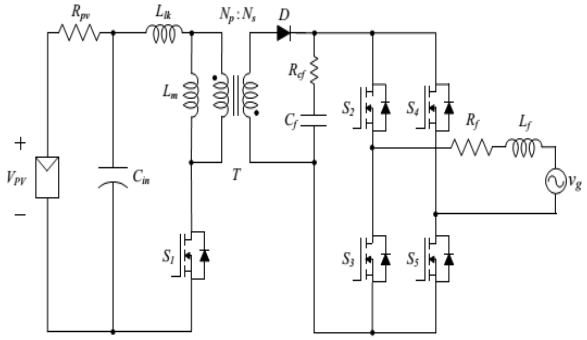

Fig. 1. The circuit diagram of flyback inverter.

The PV current is drawn from the PV panel and regulated to a full wave rectified sinusoidal waveform by high frequency switching. The H-bridge is used to mitigates the output ac current into the grid.

Photovoltaics (PV) system is used to convert sun light electrical energy to electrical energy. PV system is used mostly because it is available in free of nature.
Photovoltaics (PV) system is used to convert sun light electrical energy to electrical energy. PV system is used mostly because it is available in free of nature. The dynamic model of PV cell is appeared in below Fig.2.

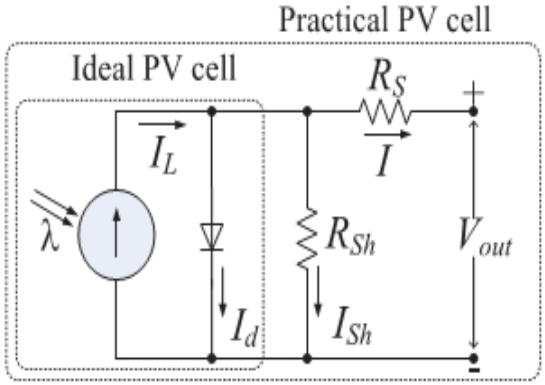

Fig 2. Equivalent electrical circuit of the PV cell.
The basic equation for the I -V characteristic of a PV cell is

$$I = I_L - I_d - I_{sh} = I_L - I_D\left[e^{\frac{QV_{oc}}{AKT}-1}\right] - \frac{V_{out}+IR_S}{R_{Sh}} \quad (1)$$

where I D is the saturation current of the diode, Q is the electron charge, A is the curve fitting constant (or diode emission factor), K is the Boltzmann

The equivalent circuit of flyback inverter is shown in fig.3.

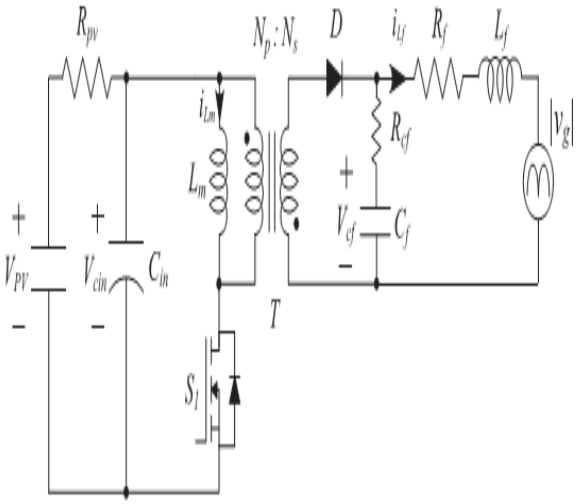

Fig. 3. The equivalent circuit of flyback inverter.
During turn-on subinterval:

$$\dot{x}(t) = \begin{bmatrix} 0 & \frac{1}{L_m} & 0 & 0 \\ \frac{1}{C_{in}} & -\frac{1}{R_{pv}C_{in}} & 0 & 0 \\ 0 & 0 & -\frac{RC_f+R_f}{L_f} & \frac{1}{L_f} \\ 0 & 0 & -\frac{1}{C_f} & 0 \end{bmatrix} x(t) + \begin{bmatrix} 0 & 0 \\ \frac{1}{R_{pv}C_{in}} & 0 \\ 0 & -\frac{1}{L_f} \\ 0 & 0 \end{bmatrix} V(t) \quad (2)$$

$$y(t) = [0 \quad 0 \quad 1 \quad 0]x(t) \quad (3)$$

During turn-off subinterval

$$\dot{X}(t) = \begin{bmatrix} -\frac{Rc_f}{n^2L_m} & 0 & \frac{Rc_f}{nL_m} & -\frac{1}{nL_m} \\ 0 & -\frac{1}{R_{pv}C_{in}} & 0 & 0 \\ \frac{Rc_f}{nL_f} & 0 & -\frac{Rc_f+R_f}{L_f} & \frac{1}{L_f} \\ \frac{1}{nC_f} & 0 & -\frac{1}{C_f} & 0 \end{bmatrix} X(t) + \begin{bmatrix} 0 & 0 \\ \frac{1}{R_{pv}C_{in}} & 0 \\ 0 & -\frac{1}{L_f} \\ 0 & 0 \end{bmatrix} v(t) \quad (4)$$

$$y(t) = [0\ 0\ 1\ 0]X(t) \quad (5)$$

where I_{Lm} is the magnetizing inductor current, V_{Cin} is capacitor voltage, I_{Lf} is the current through the output inductor, V_{Cf} is the voltage across the output capacitor. n is the transformer turns ratio of secondary to primary.

International Journal of Research
Available at https://edupediapublications.org/journals
e-ISSN: 2348-6848
p-ISSN: 2348-795X
Volume 04 Issue-17
December 2017

Problem formulation

In discrete-time domain the controller will be developed. To get a better connection between the flyback inverter system and the controller, the small signal model needs to be represented as the discrete-time transfer function.

By linearizing the averaged model, the small signal model can be derived as follows:

$$G_{id}(z) = \frac{\tilde{\imath}_{L_f}(s)}{\tilde{d}(s)} = \frac{a_1 s^3 + a_2 s^2 + a_3 s + a_4}{s^4 + b_1 s^3 + b_2 s^2 + b_3 s + b_4} \quad (6)$$

Where~I_{Lf} (t) and ~ d(t) are the small ac variations of I_{Lf} (t) and D_c(t). By analyzing the small signal model, the system has one RHP zero, two lefthalf-plane (LHP) zero, and four LHP poles.

To improve theperformance of the proposed method between the flyback inverter system and the controller. Utilizing in reverse contrast strategy with inspecting time of Ts, it can be depicted as:

$$G_{id}(z) = \frac{e_1 z^4 + e_2 z^3 + e_3 z^2 + e_4 z}{z^4 + f_1 z^3 + f_2 z^2 + f_3 z + f_4} \quad (7)$$

where the parameters ej and fj for all j =1,2,3,4 are defined.

CONTROLLER DESIGN

Conventional Controller

The working state of the flyback inverter in CCM changes gradually during a grid period contrasted with a switching period; the flyback inverter can be accepted to work in quasi steady state in every moment of the matrix time frame. By expecting semi consistent state operation and utilizing volt-second adjust for the charging inductance Lm more than one exchanging period Ts, the ostensible obligation proportion Dn(t) for flyback inverter in CCM can be acquired as [1]

$$D_n(t) = \frac{|v_g(t)|}{|v_g(t)| + nV_{pv}(t)} \quad (8)$$

Despite the fact that Dn(t) does not specifically decide the yield current, the utilization of the ostensible obligation helps the flyback inverter in CCM to create the coveted yield current by easing the impact of the unsettling influences. The exchange capacity of a state feedback controller is represented as

$$C_{fb}(z) = k_p + k_i \frac{T_s}{1 - z^{-1}} \quad (9)$$

where kp is the proportional controller gain, ki is the integral controller gain.

In this customary control plot, the RHP zero restrains the accessible controller data transfer capacity. Fig. 3 demonstrates the Bode plot of the repaid framework when the state-feedback controller is utilized.

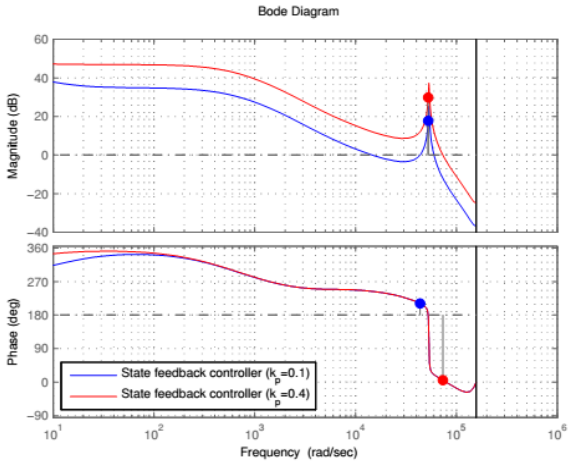

Fig. 4. The Bode plot of compensated system when the state-feedback controller is used (blue); when the high-gain state-feedback controller is used (red). The dot in each magnitude Bode plot denotes the gain margin of the compensated system. The dot in each phase Bode plot denotes the phase margin of the compensated system.

As appeared in Fig. 3, the RHP zero makes a negative phase shift between of 20 and 1kHz. In this condition, to guarantee the following execution and aggravation dismissal, for example, the grid voltage, the high-pick up state-input controller can be utilized. It would make the flyback inverter in CCM which has the RHP zero wind up plainly precarious. To defeat this issue, the dull controller is created in the continuation.

Repetitive controller with low-pass filter

The repetitive controller handles systems that performs the same task repetitively. In repetitive control scheme, to improve the control input for the next trial the knowledge obtained from the previous trial is used. Hence, the control input in each trial is adjusted using the tracking error signals obtained from the previous trial, and theoretically achieves zero tracking error. The concept of repetitive controller is shown in Fig. 4. In the conventional control scheme, the RHP zero limits the available controller bandwidth. To achieve fast dynamical response to input signal at a specific frequency, the repetitive controller is developed.

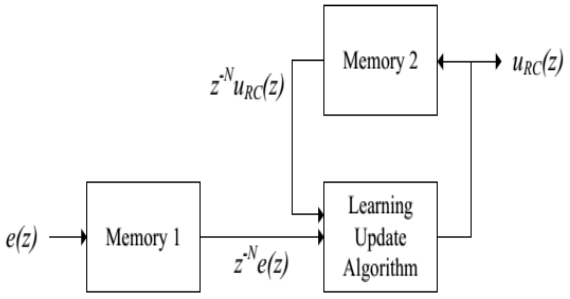

International Journal of Research
Available at https://edupediapublications.org/journals
e-ISSN: 2348-6848
p-ISSN: 2348-795X
Volume 04 Issue-17
December 2017

Fig. 5. The concept of repetitive controller

In the repetitive control scheme to allow tracking/rejecting periodic signals within a specified frequency range, a low-pass filter is adopted. Moreover, to compensate for the system delay which comes from digital implementation, the phase lead compensator is used to the repetitive controller scheme.

The transfer function of the repetitive controller is

$$C_{rc}(z) = k_r \frac{z^{-N}Q(z)}{1-z^{-N}Q(z)} G_{inv}(z) \quad (10)$$

where kr is the repetitive controller gain, N = fs/fg with fs = 1/Ts being the sampling frequency and fg being the frequency of reference, Q(z) is the low-pass filter, and Ginv(z) is the inverse function of the system. For tracking/rejecting periodic signals within a specified frequency range and easy implementation, Q(z) is chosen as moving average filter with zero phase shift:

$$Q(z) = \sum_{i=0}^{p} \alpha_i z^i + \sum_{i=1}^{p} \alpha_i z^{-i} \quad (11)$$

where it is the number of samples to be used for filtering. Here, a first order filter Q(z) = α1z +α 0 + 1zα1 is used; as 0 becomes larger, the cutoff frequency of Q(z) becomes higher. Due to the system uncertainty, the system delay, and the unknown disturbance, $G_{inv}(z)$ cannot be precisely implemented. Here, to compensate even the effect of the system delay, G_{inv} are set as

$$G_{inv}(z) = z^m \quad (12)$$

where m is the prediction index. With the complete repetitive controller, the overall control system is shown in Fig. 5.

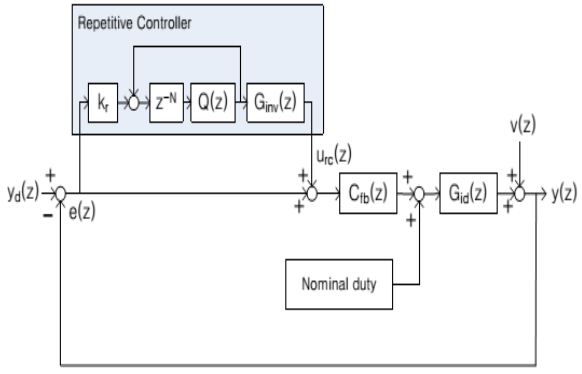

Fig. 6. The schematic diagram of overall control system. yd(z) is the reference, e(z) is the error, urc(z) is the repetitive control input, v(z) = [Vpv(z); jvg(z)j]T .

Fig. 6 demonstrates the Bode plot of the compensated system when the repetitive controller is utilized. Utilized parameters are recorded in Table I. To maintain a strategic distance from the control at a high-recurrence and stifle crucial and low-arrange music parts, the low-pass channel is received in the monotonous control conspire. It cripples the learning at high-recurrence.

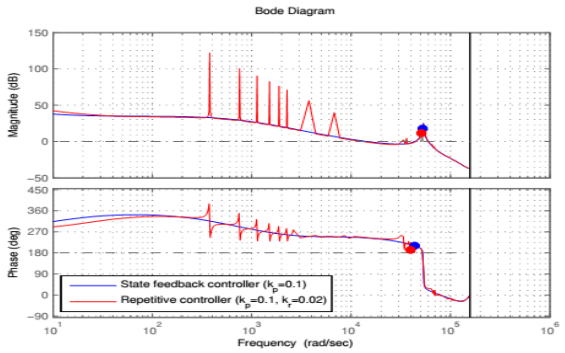

Fig.7. The Bode plot of compensated system when the state-feedback controller is used (blue); when the repetitive controller with low-pass filter is used (red). The dot in each magnitude Bode plot denotes the gain margin of the compensated system. The dot in each phase Bode plot denotes the phase margin of the compensated system.

Stability Analysis

In the repetitive control system shown in Fig. 5, the inputoutput relationship of the flyback inverter in CCM is described as

$$y(z) = G(z)y_d(z) + S(z)v(z) \quad (13)$$

where G(z)yd(z) is the command input response and S(z)v(z) is the disturbance response; G(z) is the transfer function from reference to output and S(z) is the sensitivity function; G(z) and S(z) are represented as

$$G(z) = \frac{y(z)}{yd(z)} = \frac{[1-Q(z)z^{-N}(1-k_r z^m)]G_C(Z)}{[[1-Q(z)z^{-N}(1-k_r z^m)]G_C(Z)]}$$

$$S(z) = \frac{y(z)}{u(z)} = \frac{[1-Q(z)z^{-N}](1-G_C(Z))}{1-Q(z)z^{-N}(1-k_r z^m G_C(Z))} \quad (14)$$

where Gc(z) = Cfb(z)Gid(z)=(1 + Cfb(z)Gid(z)). The relationship between the error e(z) = y(z) - yd(z) and the reference yd(z) and disturbance v(z) can be obtained as

$$\frac{e(z)}{w(z)} = \frac{(1-Q(z)z^{-N})(1-G_C(Z))}{1-Q(z)z^{-N}(1-k_r z^m G_c(z))} \quad (15)$$

The transfer function e(z)/w(z) can be written as three systems connected in cascade. The term 1 - Q(z)z $^{-N}$ is a low-pass filter and a time delay, and so it is stable.

INCREMENTAL CONDUCTANCE MPPT

In incremental conductance method the array terminal voltage is always adjusted according to the MPP voltage it is based on the incremental and instantaneous conductance of the PV module.

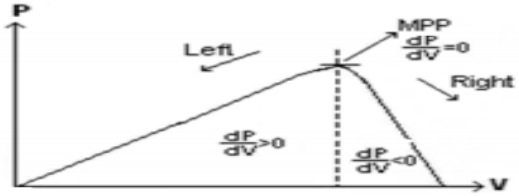

International Journal of Research
Available at https://edupediapublications.org/journals
e-ISSN: 2348-6848
p-ISSN: 2348-795X
Volume 04 Issue-17
December 2017

Fig-8: Basic idea of incremental conductance method on a P-V Curve of solar module

Fig-6 shows that the slope of the P-V array power curve is zero at the MPP, increasing on the left of the MPP and decreasing on the Right-hand side of the MPP. The basic equations of this method are as follows.

$$\frac{dI}{dV} = -\frac{1}{V} \; AtMPP$$

$$\frac{dI}{dV} > -\frac{1}{V} \; LeftofMPP$$

$$\frac{dI}{dV} < -\frac{1}{V} rightofMPP \qquad (16)$$

Where I and V are P-V array output current and voltage respectively. The left-hand side of equations represents incremental conductance of P-V module and the right-hand side represents the instantaneous conductance.

INCRIMENTAL CONDUCTANCE MPPT ALGORITHM

This method exploits the assumption of the ratio of change in output conductance is equal to the negative output Conductance Instantaneous conductance. We have,

$$P = VI \qquad (17)$$

Applying the chain rule for the derivative of

$$\partial P/\partial V = [\partial(VI)]/\partial V$$

$$\partial P/\partial V = 0 \qquad (18)$$

The above equation could be written in terms of array voltage V and array current I as

$$\partial I/\partial V = - I/V \qquad (19)$$

The MPPT regulates the PWM control signal of the dc – to – dc boost converter until the condition: $(\partial I/\partial V) + (I/V) = 0$ is satisfied.

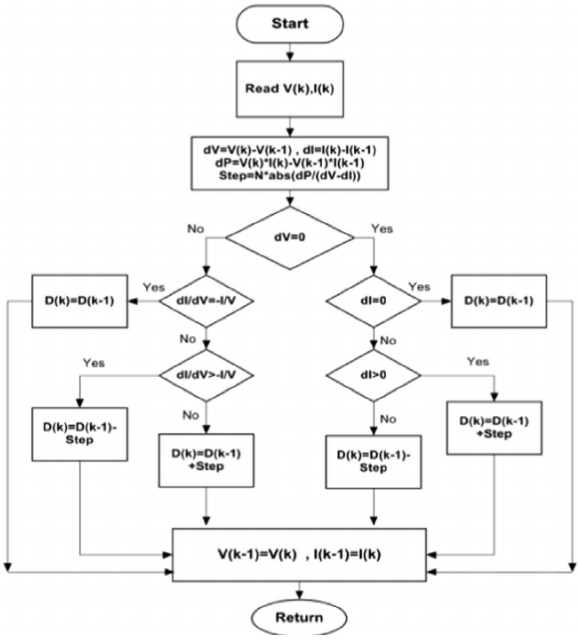

Fig. 9. Flowchart for IC MPPT of switched PV approach.

In this method the peak power of the module lies at above 98% of its incremental conductance. The Flow chart of incremental conductance MPPT is shown below.

SIMULATION RESULTS

To exhibit the performance of the proposed controller, simulation. The flyback inverter in CCM mode parameters are input voltage Vpv = 60 V, framework voltage vg = 220 Vrms, and evaluated yield control Po = 200 W. The real parameters for proposed inverter are recorded in Table I. The aggregate framework design is appeared in Fig. 10.

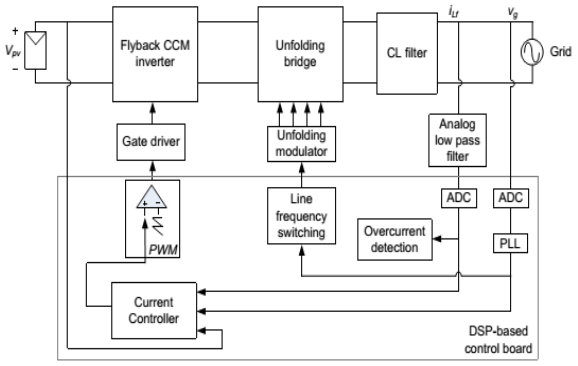

Fig. 10. Configuration of the proposed control system. PWM stands for pulsewidth modulation. ADC stands for analog-to-digital converter.

Fig. 11(a) demonstrates waveforms of the reference and yield streams when regular control plot with straight controller in addition to feedforward controller is connected.

International Journal of Research
Available at https://edupediapublications.org/journals
e-ISSN: 2348-6848
p-ISSN: 2348-795X
Volume 04 Issue-17
December 2017

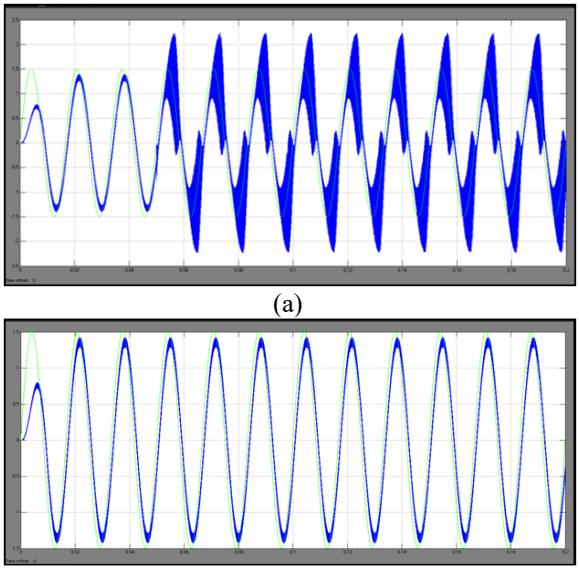

(a)

Fig. 11. The waveforms of desired output current (a) When the conventional controller is used. (b) When the proposed controller is used.

Fig. 11 b indicates waveforms of the reference and yield current when proposed control conspire is connected.

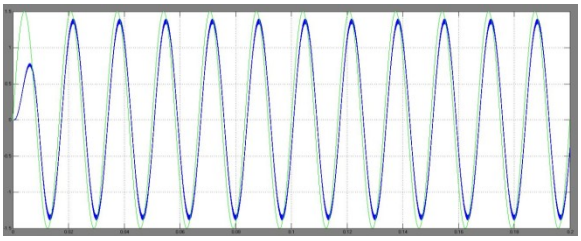

Fig.12The waveforms of desired output current

CONCLUSION

According to this paper the feedback of the output current and the utilization of the repetitive control algorithm will be applied for the PV system with the Increment condition to track the maximum power from the source to fly back inverter which is operated under CCM. Which is simple in design, minimal effort, and high effectiveness. In the incremental conductance method, the controller measures incremental changes in PV array current and voltage to predict the effect of a voltage change. To extract maximum power from module recognition of optimal operating point is important as solar photovoltaic module is nonlinear power source and output power of modules varies with temperature and insolation. To achieve the accurate tracking performance and disturbance rejection, the repetitive controller is developed which is applied to flyback inverter in CCM operation. Therefore, in order to rejecting periodic signals within a specified frequency range by utilizing the low pass filtertherefore, the zero tracking error will be achieved and stability of closed-loop system will be derivedby using the simulation we can verify the proposed control method.

REFERENCES

[1] F. F. Edwin, W. Xiao, and V. Khankikar, "Dynamic displaying and control of interleaved flyback module-incorporated converter for PV control applications," IEEE Trans. Ind. Electron., vol. 61, no. 3, pp. 1377-1388, Mar. 2014.

[2] S. B. Kjaer, J. K. Pedersen, and F. Blaabjerg, "An audit of single-stage framework associated inverters for photovoltaic modules," IEEE Trans. Ind. Appl., vol. 41, no. 5, pp. 1292-1306, Sep./Oct. 2005.

[3] Y. H. Kim, J. W. Jang, S. C. Shin, and C. Y. Won, "Weighted-proficiency upgrade control for photovoltaic AC module interleaved flyback inverter utilizing a synchronous rectifier," IEEE Trans. Power Electron., vol. 29, no. 12, pp. 6481-6493, Dec. 2014.

[4] G. Petrone, G. Spagnuolo, and M. Vitelli, "A simple system for conveyed MPPT PV applications," IEEE Trans. Ind. Electron., vol. 59, no. 12, pp. 4713-4722, Dec. 2012

. [5] Y. Li and R. Oruganti, "A flyback-CCM inverter conspire for photovoltaic AC module application," in Proc. Australasian Univ. Power Eng. Conf. (AUPEC), 2008, pp 1-6.

[6] N. Kasa, T. Iida, and L. Chen, "Flyback inverter controlled by sensorless current MPPT for photovoltaic power framework," IEEE Trans. Ind. Electron., vol. 52, no. 4, pp. 1145-1152, Aug. 2005.

[7] N. Sukesh, M. Pahlevaninezhad, and P. K. Jain, "Examination and execution of a solitary stage flyback PV microinverter with delicate exchanging," IEEE Trans. Ind. Electron., vol. 61, no. 4, pp. 1819-1833, Apr. 2014.

[8] Z. Zhang, X. F. He, and Y. F. Liu, "An ideal control strategy for photovoltaic lattice tide-interleaved flyback microinverters to accomplish high productivity in wide load extend," IEEE Trans. Power Electron., vol. 28, no. 11, pp. 5074-5087, Nov. 2013.

[9] H. Hu, S. Harb, N. H. Kutkut, Z. J. Shen, and I. Batarseh, "A singlestage microinverter without utilizing electrolytic capacitors," IEEE Trans. Power Electron., vol. 28, no. 6, pp. 2677-2687, Jun. 2013.

[10] R. W. Erickson and D. Maksimovic, "Essentials of Power gadgets," Springer Science and Business Media, 2007.